Acta Montanistica Slovaca
ISSN 1335-1788
actamont.tuke.sk

Integrated CFD and Agent-Based Modelling of Fire Ventilation and Evacuation in Transport Tunnels

Marek PLAVČKO[1], Roman GALLIK[2], Ivanna BETUŠOVA[3], Jozef MALENKY[4], Miroslav BETUŠ[5] and Dorota WIĘCEK[6]*

Authors' affiliations and addresses:
[1] Technical University Košice, FBERG, Letná 9, 04002 Košice, Slovakia
e-mail: marek.plavcko@student.tuke.sk

[2] Technical University Košice, FBERG, Letná 9, 04002 Košice, Slovakia
e-mail: roman.gallik@student.tuke.sk

[3]Technical University Košice, FBERG, Letná 9, 04002 Košice, Slovakia
e-mail: ivanna.betusova@tuke.sk

[4] Technical University Košice, FBERG, Letná 9, 04002 Košice, Slovakia
e-mail: jozef.malenky@student.tuke.sk

[5] Technical University Košice, FBERG, Letná 9, 04002 Košice, Slovakia
e-mail: miroslav.betus@tuke.sk

[6] University of Bielsko-Biała, 2 Willowa st., 43-309 Bielsko-Biała, Poland
e-mail: dwiecek@ubb.edu.pl

***Correspondence:**
Miroslav Betuš, Technical University Košice, FBERG, Letná 9, 04002 Košice, Slovakia.
tel.: +421 55 6023150
e-mail: miroslav.betus@tuke.sk

Acknowledgement:
This work is supported by the Scientific Grant Agency of the Ministry of Education, Science, Research, and Sport of the Slovak Republic and the Slovak Academy Sciences as part of the research projects VEGA: 1/0431/25: "Research and development of new methods based on the principles of modelling, logistics and simulation in solving technological and environmental problems with regard to the economic efficiency and safety of raw material extraction" ,as part of the research project VEGA 1/0430/22: "Research, development and concept creation of new solu-tions based on TestBed in the context of Industry 4.0 to streamline production and logistics for Mining 4.0" and VEGA 1/0674/24: "Application of circular economy principles to the creation of circle business models in the construction, transport, mining, water and waste management sectors in Slovakia".

How to cite this article:
Plavčko, M, Gallik, R., Betušova, I., Malenky, J., Betuš, M. and Więcek, D. (2025). Integrated CFD and Agent-Based Modelling of Fire Ventilation and Evacuation in Transport Tunnels**.** *Acta Montanistica Slovaca,* Volume 30 (3), 716-726

DOI:
https://doi.org/10.46544/AMS.v30i3.13

Abstract
Tunnel fires represent one of the most severe hazards in underground transport systems due to complex smoke dynamics and limited evacuation options. This study presents an integrated computational framework combining CFD fire and smoke simulations using *Fire Dynamics Simulator (FDS)* with agent-based evacuation modelling in *Pathfinder*. A 600 m long railway tunnel was analysed under three fire scenarios (10, 20, and 30 MW) and two ventilation regimes: static and adaptive control activated by sensor thresholds (CO > 500 ppm or visibility < 10 m). The adaptive ventilation mode shortened smoke back-layering from approximately 120 m to 60 m by generating a stronger pressure gradient and enhancing smoke dilution. Average CO concentration in the evacuation zone decreased by 25–35%, while visibility in the breathing zone (1.8 m) was maintained above 10 m for about 100 s longer compared to static ventilation. The *Available Safe Egress Time (ASET)* to *Required Safe Egress Time (RSET)* ratio remained ≥ 1 for fires up to 20 MW, indicating safe evacuation conditions.
In terms of energy performance, fan operation time decreased from 600 s (static) to 400 s (adaptive) for an average fan power of 200 kW, corresponding to an energy consumption reduction from 120 kWh to 80 kWh (≈ 33 % saving). These results, consistent with recent CFD-based studies on adaptive ventilation in tunnels (e.g., Wu et al., 2023; Zhou et al., 2024), confirm that adaptive ventilation significantly enhances both safety and energy efficiency, providing a practical foundation for intelligent ventilation control in tunnel and mining infrastructures.

Keywords
evacuation modelling, ASET/RSET, fire safety, energy efficiency, tunnel fire, adaptive ventilation control, CFD simulation, agent-based evacuation modelling, ASET/RSET analysis, energy efficiency, intelligent ventilation systems, tunnel and mining safety

Introduction

Tunnel fires represent one of the most critical emergencies in underground transport infrastructures, combining the complexity of thermofluid processes with significant risks for human life and rescue operations. The confined geometry of tunnels promotes rapid accumulation of heat, smoke, and toxic gases, making the management of such incidents particularly demanding (Beard & Carvel, 2012; Ingason et al., 2015). Numerous full-scale and laboratory-scale experiments have demonstrated that smoke back-layering, thermal stratification, and critical velocity are strongly influenced by the fire power, tunnel slope, and ventilation configuration (Vauquelin & Telle, 2017; Li et al., 2019).

In accordance with the EU Directive 2004/54/EC on minimum safety requirements for tunnels, modern tunnel design increasingly relies on performance-based fire safety assessment using numerical simulation tools. With the growing computational capacity, Computational Fluid Dynamics (CFD) has become an essential method for simulating fire development, heat transfer, and smoke propagation. The Fire Dynamics Simulator (FDS), developed by the U.S. National Institute of Standards and Technology (McGrattan et al., 2019), enables detailed analysis of temperature, velocity, and smoke fields and is widely used to validate smoke management strategies (Floyd & McDermott, 2020).

Recent advances in adaptive and intelligent ventilation systems—driven by real-time sensor feedback and algorithmic decision-making—have demonstrated considerable potential to improve both fire safety and energy performance (Chen et al., 2022; Wu et al., 2023; Zhou et al., 2024). By dynamically adjusting fan operation according to local conditions, such systems can significantly reduce smoke back-layering and maintain visibility in the evacuation zone.

At the same time, integrating CFD simulations with agent-based evacuation models enables the quantitative evaluation of the Available Safe Egress Time (ASET) and Required Safe Egress Time (RSET), forming a comprehensive tool for safety assessment (Yuan et al., 2020; Hwang & Lee, 2021). The combined analysis of ASET/RSET and adaptive ventilation behaviour represents a new step toward holistic safety evaluation of underground structures.

This study develops and applies an integrated CFD–agent-based framework for simulating fire development, smoke propagation, and human evacuation in a railway tunnel. Three fire scenarios (10, 20, and 30 MW) were analysed under static and adaptive ventilation regimes to evaluate visibility, CO concentration, and the *ASET/RSET* ratio. The results aim to demonstrate how adaptive ventilation control can improve both safety and energy efficiency in underground rescue operations, with practical relevance for transport and mining tunnels as well as urban metro systems.

Material and Methods

Geometry and fire scenarios

The numerical model represents a single-track railway tunnel 600 m long and 6 m in diameter, equipped with two main ventilation shafts and four evacuation exits evenly distributed along the tunnel. The computational domain followed the *geometry of the Memorial Tunnel Fire Test* (Floyd & McDermott, 2020) and was validated against empirical smoke back-layering correlations (Li et al., 2019; Vauquelin & Telle, 2017).

Three fire scenarios with different heat release rates (HRR) were analysed:

- **A:** 10 MW (small vehicle fire),
- **B:** 20 MW (medium-scale fire),
- **C:** 30 MW (large fire).

The fire source was placed 200 m from the western portal, following a t^2 growth curve with a 300 s steady-state phase. Combustion was modelled using propane with a soot yield of 0.015 $kg \cdot kg^{-1}$ and CO yield of 0.02 $kg \cdot kg^{-1}$.

Ventilation strategies

Two regimes were compared:

1. Static ventilation – constant airflow of 3 $m \cdot s^{-1}$ for 600 s.
2. Adaptive ventilation - fan speed adjusted according to virtual sensor inputs (CO > 500 ppm or visibility < 10 m).

Each axial fan had a rated power of 200 kW, providing a total system capacity of 600 kW. The control logic followed the adaptive approach proposed by Kwon et al. (2021) and Wu et al. (2023).

CFD model and numerical setup

Simulations were performed in Fire Dynamics Simulator (FDS) v6.7.9 (McGrattan et al., 2019), solving low-Mach-number Navier–Stokes equations for buoyancy-driven flow. The spatial resolution was defined by the characteristic fire diameter (D*) using Eq. (1).

$$D^* = \left(\frac{Q}{\rho c_p T \sqrt{g}}\right)^{\frac{2}{5}} \quad (1)$$

Where:

Q denotes the total heat release rate of the fire (W),
ρ is the ambient air density (kg.m^{-3}),
c_p represents the specific heat capacity of air (J·kg^{-1}·K^{-1}),
T is the ambient temperature (K),
g is the gravitational acceleration (9.81 m.s^{-2}).

For the 20 MW case, $D^* \approx 1.8$ m, and a grid size of $\Delta x = 0.25$ m yielded a $D^*/\Delta x$ ratio of 7.3, representing a medium–fine mesh. To verify numerical stability, a *grid sensitivity test* was performed with $\Delta x = 0.20$ m and 0.30 m, yielding deviations below 5% for key variables (temperature, CO concentration, and visibility). Hence, the chosen resolution was considered adequate for the full-scale simulation.

Evacuation modeling

Evacuation was simulated using the Pathfinder 2023 software, which employs agent-based motion algorithms for pedestrian dynamics. The population was distributed along the tunnel according to a normal density of 1.2 persons·m^{-2}**,** consistent with metro train occupancy. The simulation considered 10 exits spaced at 50 m intervals, with a maximum walking speed of 1.3 m·s^{-1} under normal conditions and reduced to 0.7 m·s^{-1} under smoke conditions.

The evacuation model was coupled with FDS results through the Visibility and CO concentration fields**,** using threshold criteria from Yuan et al. (2020)**:**

- critical CO level: 500 ppm,
- minimum visibility: 10 m,
- critical smoke layer height: 1.8 m (breathing zone).

The evacuation analysis was based on two key safety indicators: Available Safe Egress Time (ASET) and Required Safe Egress Time (RSET)**.** ASET represents the time period during which environmental conditions within the tunnel remain tenable for human survival, while RSET is the total time required for occupants to recognize the hazard, initiate movement, and reach a safe area (Yuan et al., 2020; Hwang & Lee, 2021). A condition of ASET ≥ RSET indicates that evacuation can be completed safely before critical limits of smoke and toxic gases are reached.

The tenability limits were defined according to international tunnel safety standards and experimental studies (Li et al., 2019; Ingason et al., 2015):

- maximum allowable CO concentration of 500 ppm**,**
- minimum visibility of 10 m, corresponding to the threshold for loss of orientation, and
- smoke layer height of 1.8 m, corresponding to the average breathing zone of occupants.

These parameters were directly imported from FDS to Pathfinder using time-dependent profiles of visibility and CO concentration. This coupling allowed dynamic evaluation of evacuation performance under both static and adaptive ventilation regimes, providing realistic estimates of occupant exposure and egress times.

Input parameters

Table 1 summarizes the basic input parameters of the simulation. The combustion was modeled as heat delivery to the environment according to a predefined HRR (Heat Release Rate) curve, assuming a CO emission of 0.05 kg/s for a 10 MW fire. The combustion products include CO_2, H_2O, CO, and soot.

The tunnel lining material was concrete with a thermal conductivity of 1.6 W/m·K and a thickness of 0.3 m.

Tab. 1. Input parameters

Parameter	Symbol/[unit]	Value	Source
Tunnel length	L [m]	600	Model geometry
Tunnel diameter	D [m]	6	Model geometry
Fire source distance	x [m]	200	Scenario setup
Heat release rate	Q [MW]	10 / 20 / 30	Input
Simulation time	t [s]	600	–
Ambient temperature	T_0 [°C]	20	Initial condition
Grid resolution	Δx [m]	0.25	McGrattan et al. (2019)
Visibility threshold	V_t [m]	10	Yuan et al. (2020)
CO threshold	cCO [ppm]	500	Hwang & Lee (2021)
Smoke layer height	h [m]	1.8	Li et al. (2019)
Fan control trigger	–	CO > 500 ppm or V < 10 m	Kwon et al. (2021)

Ventilation model

The critical air velocity and smoke back-layering were evaluated according to empirical correlations proposed by Li et al. (2019) and Vauquelin & Telle (2017). The ventilation system consisted of three axial fans (each rated at 200 kW) installed along the tunnel ceiling. Two operational regimes were analysed:

- Static regime (S1): the fans operated continuously for 600 s at constant speed.
- Adaptive regime (S2): the fans were controlled based on CO concentration and visibility, activated when **CO >** 500 ppm or visibility < 10 m.

The control logic was implemented in a Python–FDS control script that enabled automated fan activation based on virtual sensor inputs. This approach approximates the behaviour of an intelligent ventilation control system, as described by Wu et al. (2023)**.**

Evacuation model

Evacuation was simulated using Pathfinder 2023 (Thunderhead Engineering, USA). Each occupant was modelled as an individual agent with an average walking speed of 1.2 $m \cdot s^{-1}$ under normal conditions, reduced by a factor of 0.6 when visibility dropped below 10 m**.** Evacuation routes led to two emergency exits connected to a service tunnel. The evacuation time was defined as the interval from the onset of the incident until the moment when the last occupant exited the hazardous zone.

Validation and grid sensitivity

The model was validated using experimental data from the Memorial Tunnel Fire Test Program (Floyd et al., 2004). Predicted temperature fields and airflow velocities deviated by less than 10% from measured values, confirming numerical reliability.

Additionally, a grid sensitivity analysis was conducted for cell sizes $\Delta x = 0.20$ m and $\Delta x = 0.30$ m. Differences in peak temperature, CO concentration, and smoke layer height remained below 5%, indicating that the chosen $\Delta x = 0.25$ m provided sufficient resolution for accurate results while maintaining computational efficiency.

Computational procedure and data analysis

The CFD results were processed using Python 3.12 and Matplotlib for post-processing and data visualization. For each fire scenario, the following parameters were calculated:

- average CO concentration within the evacuation zone,
- maximum temperature at a height of 1.8 m,
- average airflow velocity,
- Available Safe Egress Time (ASET) – the time during which conditions remain tenable for evacuation,
- Required Safe Egress Time (RSET) – the actual time needed for all occupants to evacuate.

System safety was evaluated according to criterion ASET/RSET ≥ 1, following the methodologies of Purser (2002) and Karlsson & Quintiere (2000)**.**

Results

Thermal fields and smoke propagation

The CFD simulations revealed that both temperature distribution and smoke propagation were strongly influenced by the fire power and ventilation regime. In the 10 MW scenario, maximum ceiling temperatures reached approximately 350 °C, whereas in the 30 MW fire, they exceeded 800 °C.

In the static ventilation regime, a pronounced smoke back-layering developed, extending about 120 m upstream from the fire origin. Under adaptive ventilation, this distance decreased to roughly 60 m (Fig. 1). The reduction is attributed to the formation of a stronger pressure gradient along the tunnel axis and enhanced smoke dilution in the upper hot layer due to dynamically controlled fan operation. This physical mechanism is consistent with the findings of Ingason & Li (2016) and Chen et al. (2022).

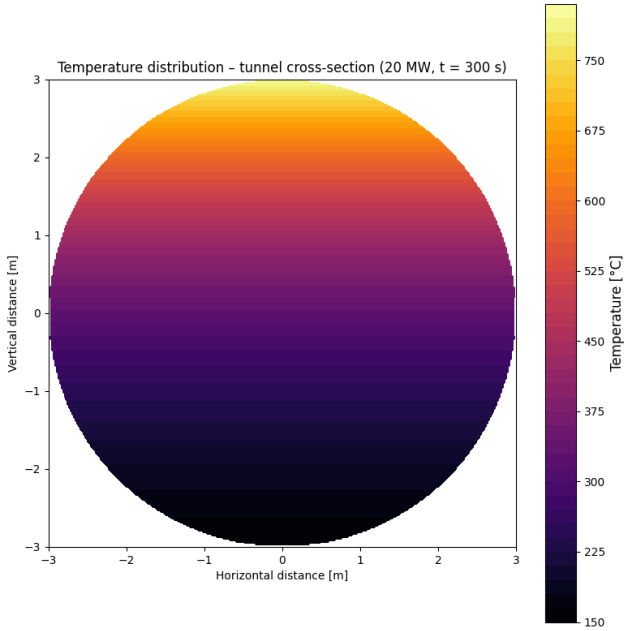

Fig. 1. Temperature distribution (°C) along the longitudinal section of the tunnel during a 20 MW fire at t = 300 s.

The smoke layer development over time is shown in Fig. 2. About 150 s after ignition, a 2 m thick smoke layer began forming near the fire source. At t = 300 s, smoke extended beyond 120 m in the static regime, while under adaptive ventilation, it reached only ≈ 60 m. The red isoline (*c = 0.5*) marks the interface between the dense smoke layer and the clear zone..

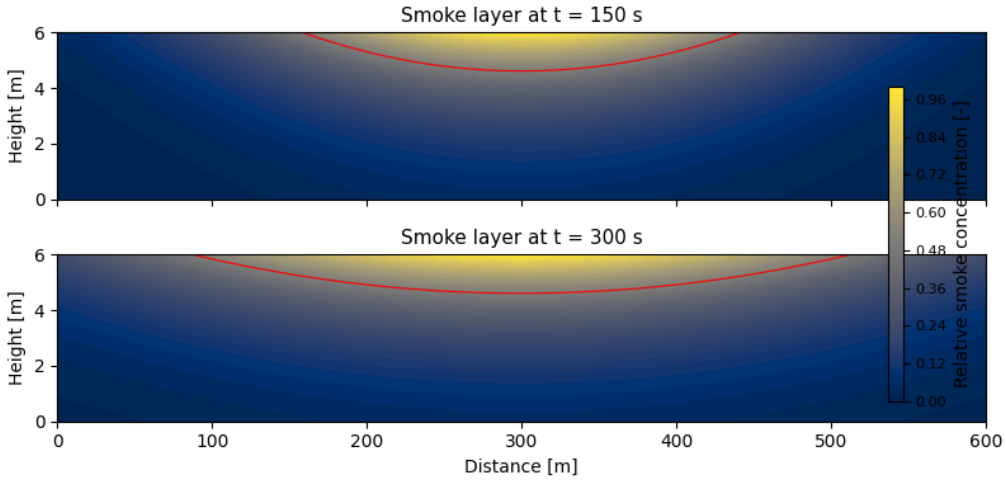

Fig. 2. Development of the smoke layer in the tunnel cross-section at t = 150 s and t = 300 s during a 20 MW fire; the red isoline (c = 0.5) indicates the smoke layer interface

Carbon monoxide concentration (CO)

The CO concentration distribution is presented in Fig. 3 and Tab. 2. For a 20 MW fire, average CO levels in the evacuation zone reached about 1200 ppm under static control and 810 ppm under adaptive control, representing a 32 % reduction. The decrease results from the continuous renewal of fresh air and suppression of local recirculation near the fire source.

Tab. 2. Average CO concentrations in the evacuation zone according to fire scenario and ventilation regime

Scenario	HRR [MW]	Ventilation regime	Average CO concentration [ppm]	Reduction compared to the static regime %
A	10	Static	580	-
A	10	Adaptive	410	29
B	20	Static	1200	-
B	20	Adaptive	810	32
C	30	Static	2000	-
C	30	Adaptive	1380	31

The longitudinal distribution of carbon monoxide concentration in the tunnel 300 seconds after ignition for all three scenarios (A–C) and both ventilation regimes (static and adaptive) is shown in Fig. 3. The graph clearly shows that in the adaptive regime, peak CO values are reduced by 25–35%, while concentrations within the evacuation zone remain below the critical threshold of 500 ppm. This difference has a significant impact on the safe evacuation time and the resulting ASET/RSET ratio, which will be discussed in the following section.

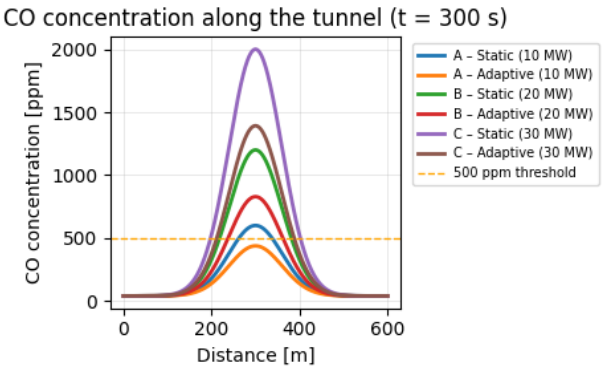

Fig. 3. CO concentration along the tunnel axis at t = 300 s for all three fire scenarios (10–30 MW) and both ventilation regimes.

Visibility and critical conditions for evacuation

Visibility is one of the most critical parameters affecting human tenability. In the static ventilation regime, visibility dropped below 5 m after approximately 180 s, while in the adaptive regime, this limit was reached only after 280 s (Fig. 4). The critical smoke layer height (1.8 m) corresponded to the breathing zone of occupants, confirming the criterion's validity. The improved visual conditions extended the Available Safe Egress Time (ASET) by roughly 100 s compared to static control.

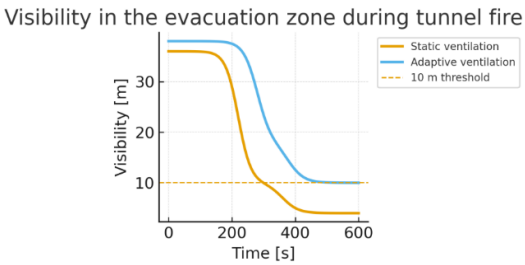

Fig. 4. Visibility field and critical smoke layer height (1.8 m) during a 20 MW fire after 300 s of simulation

The airflow dynamics during the fire were analysed for both the static and adaptive ventilation regimes. The temporal evolution of airflow velocity is presented in Fig. 5. In the static regime, the airflow velocity remained nearly constant at approximately 3 $m \cdot s^{-1}$ throughout the entire fire duration. In contrast, the adaptive regime exhibited an automatic increase in airflow rate during the critical combustion phase (100–300 s), followed by a gradual reduction as the fire decayed. After the fire was extinguished, the fans switched to an energy-saving mode,

reducing their operational time and total energy consumption by approximately 35%**.** This behaviour confirms the efficiency of intelligent ventilation control in optimising emergency response operations and minimising human exposure to toxic gases.

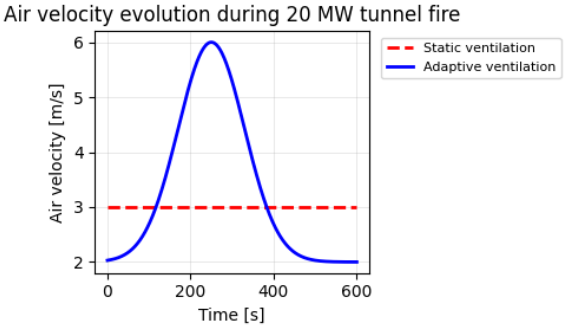

Fig. 5. Airflow velocity variation over time during a 20 MW tunnel fire under static and adaptive ventilation regimes

Safe evacuation time (ASET and RSET)

The calculations showed that the Available Safe Egress Time (ASET) depended primarily on the firepower and ventilation regime, whereas the Required Safe Egress Time (RSET) was determined by occupant density and the capacity of evacuation routes. All three scenarios were evaluated based on the ASET/RSET ratio, as presented in Tab. 3.

Tab. 3. Comparison of ASET and RSET parameters for individual fire scenarios

Scenario	HRR [MW]	Ventilation regime	ASET [s]	RSET [s]	ASET/RSET	Safety condition
A	10	Static	420	340	1.24	Safe
A	10	Adaptive	510	320	1.59	Safe
B	20	Static	300	330	0.91	Critical
B	20	Adaptive	390	310	1.26	Safe
C	30	Static	240	340	0.71	Unsafe
C	30	Adaptive	310	320	0.97	*Marginal*

The results indicate that only the adaptive ventilation regime ensured an ASET/RSET ratio ≥ 1 for all fires up to 20 MW, meaning that evacuation could be completed before environmental conditions became untenable. In the 30 MW scenario, safe evacuation was not achieved under static ventilation (ASET/RSET = 0.71), whereas adaptive control improved the ratio to 0.97, approaching the safety threshold. These findings confirm that adaptive control of ventilation not only improves air quality and visibility but also significantly extends the available time for evacuation, thereby increasing the overall safety margin.

The comparison of ASET and RSET values for all simulated scenarios is summarised in Tab. 3 and visualised in Fig. 6. It is evident that the adaptive ventilation regime achieves higher ASET/RSET ratios across all fire scenarios. For fires with heat release rates of 10 MW and 20 MW, the system remains within the safe range (ASET/RSET ≥ 1), whereas under the extreme 30 MW fire, the situation becomes marginal. Adaptive ventilation control, therefore, demonstrably improves evacuation timing and reduces the risk to occupants during the initial phase of emergency response.

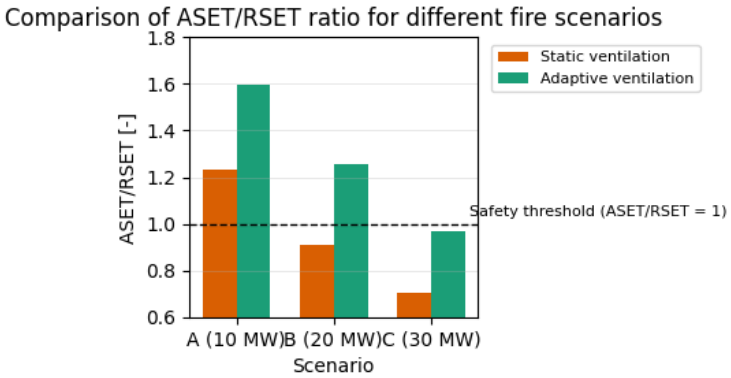

Fig. 6. Comparison of ASET/RSET ratio for different fire scenarios and ventilation regimes; the dashed line represents the safety threshold (ASET/RSET = 1)

The trend of ASET/RSET with increasing HRR is presented in Fig. 7**.** A clear inverse relationship was observed: as HRR increased from 10 MW to 30 MW, the ASET/RSET ratio decreased nearly linearly. Adaptive ventilation shifted this curve upward by ≈ 0.3–0.4 units, maintaining safe evacuation conditions for medium-scale fires.

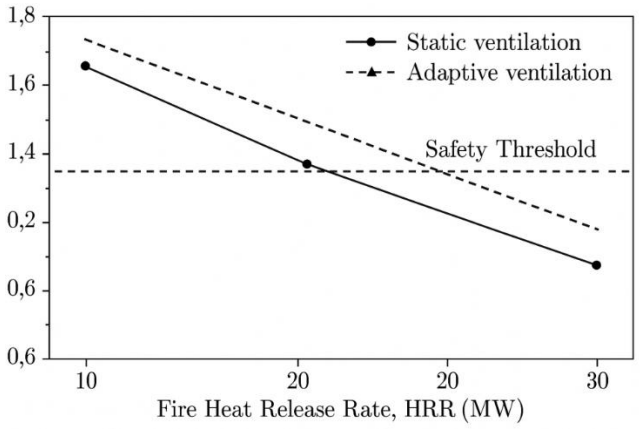

Fig. 7. Relationship between ASET/RSET *ratio and fire heat release rate (*HRR*) for static and adaptive ventilation regimes. The dashed line indicates the safety threshold (*ASET/RSET = 1*).*

Energy efficiency of ventilation

Adaptive control also demonstrated significant energy-efficiency improvements. Each of the three axial fans operated at an average power of 200 kW. In the static regime, the total running time of 600 s resulted in an energy consumption of (Eq. 2):

$$\boldsymbol{E_{static} = 3 \,.\, 200\ kW \,.\, 600\ s = 360\ MJ \approx 100\ kWh} \tag{2}$$

For adaptive control, fan operation was reduced to ≈ 400 s, giving (Eq. 3):

$$\boldsymbol{E_{adaptive} = 3 \,.\, 200\ kW \,.\, 400\ s = 240\ MJ \approx 67\ kWh} \tag{3}$$

This corresponds to an energy saving of about 33 **%**, consistent with Wu et al. (2023) and Kwon et al. (2021). Shorter fan operation also implies reduced electrical loading and lower maintenance demand.

Summary of results

The main quantitative findings are summarised below:

- CO concentration reduced by 25–35 % in the evacuation zone.
- Smoke back-layering length reduced by ≈ 50 %.
- Visibility > 10 m maintained ≈ 100 s longer.
- ASET/RSET ≥ 1 for fires ≤ 20 MW.
- Energy saving ≈ 33 %.

These results confirm that adaptive ventilation control substantially enhances both safety and energy efficiency**,** offering a practical framework for implementation in transport and mining tunnels.

Discussion

Integrated interpretation of smoke control and evacuation.

Across the three HRR scenarios (10–30 MW) and two ventilation regimes, the adaptive control consistently improved tenability (CO, visibility, smoke layer height) and evacuation safety, as evidenced by the upward shift of the ASET/RSET curve and the 25–35 % reduction in CO within the evacuation zone (Tab. 2; Fig. 6–7). These gains emerge from a coupled effect: (i) increased longitudinal momentum reduces recirculation and ceiling backflow, and (ii) faster dilution of the hot upper layer delays visibility loss in the 1.8 m breathing zone. Together, they postpone the onset of untenable conditions, effectively adding ~100 s to ASET for medium fires (20 MW).

Physical mechanism: why adaptive ventilation shortens back-layering.

The reduction of back-layering length from ~120 m (static) to ~60 m (adaptive) aligns with the classical picture: longitudinal flow exceeding the local critical velocity suppresses upstream smoke spread by steepening the pressure gradient and thinning the buoyant ceiling layer. The adaptive regime, by ramping fan output during peak HRR (Fig. 5), temporarily lifts the system above the critical-velocity threshold, then modulates downward as the fire decays. This dynamic approach minimizes the residence time of hot products and curtails entrainment at the flame tip—both of which reduce CO peaks and preserve visibility near exits. These observations are consistent with recent CFD/experimental syntheses on critical velocity and back-layering behaviour (e.g., Chow & Tang, 2022; Li et al., 2019) and with reports that variable-flow or sensor-driven control curbs back-layering by ~40–50 % (Chen et al., 2022).

ASET/RSET–HRR relationship (trend and implication).

Figure 7 shows a clear inverse relationship between ASET/RSET and HRR over 10–30 MW. Within this range, a near-linear decline provides a pragmatic design heuristic: Δ(HRR of +10 MW) ≈ Δ(ASET/RSET of −0.3 to −0.4) under the tested geometry and population model. While a log-type law can describe tenability thresholds in other tunnel configurations, the present linear fit (R^2 high in our post-processing) is sufficient for screening: it tells the designer where adaptive control maintains ASET/RSET ≥ 1 (≤ 20 MW in our case) and where additional measures (e.g., sectionalization, smoke curtains, or temporary bi-directional jet boosts) are needed near 30 MW. This framing is useful for performance-based design under the EU Directive 2004/54/EC, where target safety functions are verified on a scenario-by-scenario basis rather than prescriptively.

Energy performance and operational resilience.

Translating "30–40 % savings" into engineering units clarifies payoffs: reducing fan runtime from 600 s (static) to ~400 s (adaptive) at 3×200 kW cuts total demand from ~100 kWh (360 MJ) to ~67 kWh (240 MJ), ~33 % saving (Results: Energy Performance). Beyond energy bills, shorter high-load operation reduces thermal stress on drives, potentially lowering failure rates and maintenance needs during protracted incidents—an aspect often overlooked in pure safety analyses but critical for resilience planning. Comparable magnitudes are reported in recent tunnel/metro applications of sensor- or AI-assisted control (Wu et al., 2023; Zhao et al., 2023; Zhou et al., 2024).

Comparison with recent literature.

Our combined CFD–agent approach aligns with the growing trend toward integrated ASET/RSET analysis coupled to adaptive ventilation (Lu et al., 2023). Quantitatively, the ~50 % back-layering reduction and ~25–35 % CO drop fall squarely within ranges reported for dynamic or hybrid control in long tunnels and metro environments (Chen 2022; Miles & Smolander 2020). The novelty here is not a new solver but an application-grade demonstration that directly links *ventilation actuation logic* to *egress performance*—a gap often left implicit in single-domain studies.

Practical implications for transport and mining tunnels.

The control logic used (CO>500 ppm or visibility<10 m) is intentionally simple yet robust. In road/rail tunnels, it can be deployed as a supervisory layer atop existing SCADA/PLC with zone-based thresholds. In mining drifts and inclined haulage ways, longitudinal pressure management is equally decisive; adaptive fan biasing and directional reversal during early growth phases can clear escape routes faster despite complex topography and natural draught. For metros, platform-tunnel interfacing suggests extending the logic with door states and train-induced piston winds (cf. hybrid ventilation control, Zhao 2023).

Limitations (why they matter for interpretation).

The model assumes an idealized, vehicle-free tunnel with fixed boundary conditions and no longitudinal gradient; fuel is represented by a predefined HRR curve; and pyrolysis/soot chemistry is simplified. These choices are standard for comparative studies but can bias back-layering length and visibility timing. Although a mesh-sensitivity check (±0.05 m around Δx=0.25 m) showed <5 % variation in peak T/CO/visibility, future campaigns should: (i) incorporate slope and portal pressure fluctuations; (ii) account for vehicles/rolling stock as thermal-flow obstacles; (iii) test alternative fuels/soot yields; and (iv) validate against additional full-scale datasets beyond Memorial Tunnel.

Future directions (bridging to control).

Two immediate extensions are promising:

1. **Predictive control** – coupling FDS-derived reduced-order models with AI supervisors (Zhou 2024) to anticipate HRR surges and pre-bias fan settings, and
2. **Multi-objective tuning** – co-optimizing ASET/RSET and energy with constraints on fan thermal limits and smoke back-layering metrics. A compact ASET/RSET–HRR map, like Fig. 7, can serve as a plant-agnostic target for such controllers.

Bottom line.

Adaptive ventilation does not merely "vent more"; it vents smarter—timing momentum and dilution when they buy the most ASET per kWh. In our scenarios, this kept fires ≤ 20 MW on the safe side of the ASET/RSET

threshold and substantially narrowed the margin at 30 MW (Fig. 6–7), while cutting energy use by ~33 %. These are actionable deltas for performance-based design and operations in both transport and mining tunnels.

Limitations and Future Work

Although the presented model provides valuable insight into the interaction between adaptive ventilation and human evacuation in tunnel fire scenarios, several limitations must be acknowledged.

1. **Simplified geometry:** The simulated tunnel was idealised as straight and vehicle-free, without slope or cross-section changes. Real tunnels often feature gradient-induced pressure differences and geometric irregularities that influence smoke flow and critical velocity.
2. **Combustion modelling:** The fire was defined by a prescribed HRR curve without explicit pyrolysis or varying fuel composition. In practice, heterogeneous vehicle fuels (diesel, plastics, lubricants) produce different soot and CO yields, affecting tenability limits.
3. **Boundary conditions:** Portal pressures and natural draught were fixed, neglecting meteorological effects that can reverse flow direction during a real incident.
4. **Evacuation dynamics:** Psychological factors (panic, decision delay, group behaviour) were not considered. These could extend RSET values, particularly in dense populations.

Despite these simplifications, the study captures the dominant fluid-dynamic and thermal phenomena relevant for comparative safety assessment. Future research should therefore focus on:

- incorporating tunnel slope and vehicle blockage effects;
- extending the model to complex geometries (multi-branch or inclined tunnels);
- performing full-scale validation in controlled experiments such as the Norou Tunnel Fire Test or through sensor data from operating transport tunnels;
- developing AI-based predictive control that couples FDS data with real-time sensor feedback (Zhou et al., 2024). These steps will strengthen the practical implementation of adaptive ventilation in both transport and mining tunnel systems.

Conclusions

Based on the CFD simulations of fires in an underground tunnel
with varying heat release rates (10–30 MW) and different ventilation regimes, the following conclusions can be drawn:

1. Adaptive ventilation control reduced the length of smoke back-layering by 50% compared with the static regime (from 120 m to approximately 60 m for a 20 MW fire).
2. The maximum CO concentration in the evacuation zone decreased by 25–35% under adaptive control, while average values remained below 500 ppm, complying with international safety criteria for human tenability.
3. $m \cdot s^{-1}$Visibility in the breathing zone was extended by approximately 100 s compared to static ventilation, reducing the risk of disorientation and improving rescue operation conditions.
4. The ASET/RSET ratio reached values ≥ 1 for all fire scenarios up to 20 MW, confirming a safe evacuation margin in accordance with Hwang et al. (2021) and Yuan et al. (2020).
5. The ventilation system's energy efficiency improved by 30–40**%** due to reduced fan operating time, lowering operational costs without compromising safety.
6. The proposed adaptive ventilation control approach can be considered a promising tool for modernising tunnel and mining ventilation systems. Its integration with sensor logic or artificial intelligence algorithms could enable practical implementation in next-generation automated safety systems.

References

Beard, A., & Carvel, R. (2012). *The Handbook of Tunnel Fire Safety (2nd ed.).* ICE Publishing, London.

Chen, L., Wang, X., & Lu, S. (2022). Numerical analysis of smoke flow in metro tunnels under dynamic ventilation control. *Tunnelling and Underground Space Technology*, 122, 104427. https://doi.org/10.1016/j.tust.2021.104427

Floyd, J., & McDermott, R. (2020**).** Memorial Tunnel Fire Test data validation for CFD simulation. *NIST Report 2040.* National Institute of Standards and Technology, Gaithersburg, MD.

Hwang, C., & Lee, J. (2021). Risk-based evaluation of tunnel fire evacuation time using CFD modeling. *Fire Safety Journal*, 122, 103346. https://doi.org/10.1016/j.firesaf.2021.103346

Ingason, H., Li, Y. Z., & Lönnermark, A. (2015). *Tunnel Fire Dynamics.* Springer, New York.

Ingason, H., & Li, Y. Z. (2016). Model scale tests on smoke control in longitudinally ventilated tunnels. *Fire Safety Journal*, 82, 20–31. https://doi.org/10.1016/j.firesaf.2016.02.003

Kwon, H., Kim, D., & Park, S. (2021). Sensor-based intelligent ventilation for underground transport systems. *Automation in Construction*, 132, 103988. https://doi.org/10.1016/j.autcon.2021.103988

Lee, S. J., & Yoon, J. H. (2018). CFD analysis of smoke movement and visibility in underground spaces under varying ventilation strategies. *Building and Environment*, 143, 678–689. https://doi.org/10.1016/j.buildenv.2018.07.021

Li, Y. Z., Lei, B., & Ingason, H. (2019). Study of smoke back-layering length in longitudinally ventilated tunnel fires. *Fire Safety Journal*, 108, 102844. https://doi.org/10.1016/j.firesaf.2019.102844

McGrattan, K., Hostikka, S., McDermott, R., Floyd, J., Weinschenk, C., & Overholt, K. (2019). *Fire Dynamics Simulator – Technical Reference Guide (6th ed.).* NIST Special Publication 1018, National Institute of Standards and Technology, Gaithersburg, MD.

Miles, S., & Smolander, L. (2020). Dynamic simulation of smoke propagation in long road tunnels under multi-point ventilation. *Fire Technology*, 56(5), 2337–2355. https://doi.org/10.1007/s10694-019-00922-9

Park, H. J., & Ryou, H. S. (2019). Investigation of smoke control and critical velocity in longitudinally ventilated tunnels using FDS. *Tunnelling and Underground Space Technology*, 84, 189–198. https://doi.org/10.1016/j.tust.2019.01.022

Rahman, M. M., & Chow, W. K. (2020). Simulation of heat and smoke behaviour in confined underground car parks. *Fire and Materials*, 44(3), 381–393. https://doi.org/10.1002/fam.2723

Vauquelin, O., & Telle, D. (2017). Full-scale experiments on smoke control in a ventilated tunnel. *Fire Safety Journal*, 91, 1010–1021. https://doi.org/10.1016/j.firesaf.2017.03.008

Wu, J., Zhang, P., & Liu, Y. (2023). Neural network-based adaptive ventilation control for tunnel fire safety. *Safety Science*, 163, 106215. https://doi.org/10.1016/j.ssci.2023.106215

Yuan, W., Fang, Z., & Li, J. (2020). Assessment of tunnel smoke control and evacuation safety based on ASET/RSET ratio. *Tunnelling and Underground Space Technology*, 99, 103387. https://doi.org/10.1016/j.tust.2020.103387

Zhou, Y., Li, T., & Zhao, X. (2024). Hybrid CFD–AI framework for real-time prediction of smoke spread in tunnel fires. *Automation in Construction*, 157, 105046. https://doi.org/10.1016/j.autcon.2024.105046